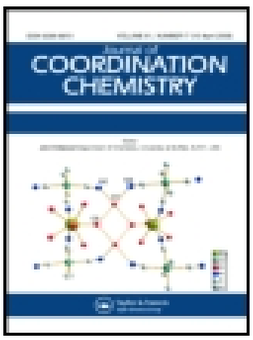

Journal of Coordination Chemistry

ISSN: 0095-8972 (Print) 1029-0389 (Online) Journal homepage: http://www.tandfonline.com/loi/gcoo20

Syntheses, structures and electrochemical properties of ruthenium(II/III) complexes with tetradentate Schiff base ligands

Jiao Ji, Xin Chen, Chang-Jiu Wang, Ai-Quan Jia & Qian-Feng Zhang

To cite this article: Jiao Ji, Xin Chen, Chang-Jiu Wang, Ai-Quan Jia & Qian-Feng Zhang (2019): Syntheses, structures and electrochemical properties of ruthenium(II/III) complexes with tetradentate Schiff base ligands, Journal of Coordination Chemistry, DOI: 10.1080/00958972.2019.1566541

To link to this article: https://doi.org/10.1080/00958972.2019.1566541

Syntheses, structures and electrochemical properties of ruthenium(II/III) complexes with tetradentate Schiff base ligands

JIAO JI, XIN CHEN, CHANG-JIU WANG, AI-QUAN JIA and QIAN-FENG ZHANG*

Institute of Molecular Engineering and Applied Chemistry, Anhui University of Technology, Ma'anshan, Anhui 243002, P R China

Three unsymmetrical tetradentate Schiff base ligands, H_2salipn, H_2salipn-Br_4 and H_2salipn-Cl_2, have been synthesized from the typical condensation reactions of treating 1,2-diaminopropane with salicylaldehyde, 3,5-dibromosalicylaldehyde and 5-chlorosalicylaldehyde, respectively. Treatment of $[RuCl_2(PPh_3)_3]$ with one equivalent of H_2salipn or H_2salipn-Br_4 in the presence of triethylamine in tetrahydrofuran (THF) afforded the corresponding ruthenium(III) complexes $[Ru^{III}Cl(PPh_3)$(salipn)] (**1**) and $[Ru^{III}Cl(PPh_3)$(salipn-Br_4)] (**2**). Interaction of $[RuHCl(CO)(PPh_3)_3]$ with one equivalent of H_2salipn-Cl_2 or H_2salipn-Br_4 under the same conditions led to isolation of ruthenium(II) complexes $[Ru^{II}(CO)(PPh_3)$(salalipn-Cl_2)] (**3**) and $[Ru^{II}(CO)(PPh_3)$(salalipn-Br_4)] (**4**), respectively, in which one of the imine bonds was nucleophilically attacked by hydride to result in the formation of a mixed imine-amine ligand. The molecular structures of **1**·1.5CH_2Cl_2, **2**, **3**·0.5CH_2Cl_2 and **4** have been determined by single-crystal X-ray crystallography. The electrochemical properties of **1**-**4** were also investigated. Their cyclic voltammograms displayed quasi-reversible Ru(IV)/Ru(III) and Ru(III)/Ru(II) couples with E^o ranging from 0.67 to 1.05 V and –0.74 to –0.80 V *vs.* Ag/AgCl (0.1 M), respectively.

Keywords: Ruthenium complex; Schiff base; Salen; Synthesis; Crystal structure; Electrochemistry

1. Introduction

In recent years, there has been considerable interest in the rational design and synthesis of Schiff base-based transition metal complexes which can be used as homogeneous catalysts for many organic transformations [1-3]. In this area, the ruthenium complexes containing N_2,O_2-tetradentate Schiff bases have been well documented. For example, Che and coworkers reported a series of (Schiff base)ruthenium complexes $[Ru^{II}$(Schiff base)$(PPh_3)_2]$, prepared by

*Corresponding author. Email: zhangqf@ahut.edu.cn

treating $[RuCl_2(PPh_3)_3]$ with tetradentate H_2(Schiff base) ligands in refluxing methanol solution containing triethylamine [4]. $[Ru^{III}Br(Nap\text{-}o\text{-}phd)(PPh_3)]$ was obtained by reaction of $[Ru^{III}Br_3(PPh_3)_2(MeOH)]$ with tetradentate Schiff base ligand (H_2Nap-*o*-phd) in a 1:1 molar ratio (H_2Nap-*o*-phd = *N*,*N*′-bis(2-hydroxy-1-naphthaldehyde) *o*-phenylene diamine) [5]. Nakajima and coworkers reported the structure of $[Ru^{III}Cl(PPh_3)(salcyn)]$ (H_2salcyn = *N*,*N*′-disalicylidene-(*R*,*R*)-1,2-cyclohexanediamine) from sequential reactions of salicylaldehyde, (*R*,*R*)-1,2-cyclohexanediamine and $[Ru^{II}Cl_2(PPh_3)_3]$ in the presence of triethylamine and air, which involved the oxidation of ruthenium(II) to ruthenium(III) by air [6]. This oxidation phenomenon was also reported by the Che, Sessoli and Ouahab research groups, who found that the coordinated chloride of $[Ru^{III}(salen)(PPh_3)(Cl)]$ was labile and easily underwent substitution in the presence of Ag(I) (where $salen^{2-}$ = *N*,*N*-ethan-1,2-diylbis(salicylidenamine) [7-9]. The N_2,O_2-tetradentate Schiff base ligands in the above results usually chelate with the ruthenium center forming a stable co-planar RuN_2O_2 square. However, as shown in chart 1, when one of the imine groups is reduced to amine, the resulting salalen ligand will not coordinate to metals facially due to steric effects. Instead, the salalen ligand adopts a *cis*-β configuration in its complexes [10]. Actually, several *cis*-β metal(ONNO) complexes have been prepared, such as $[Fe(OMe)(salalphen)]_2$ [11], Ni(salalcyn) [12], $Mo(O)_2$(salalcyn-$^tBu_2$) [13] and $[Re(O)(PPh_3)(salalphen)](PF_6)$ [14]. Previously, we have synthesized and characterized several ruthenium(II)/ruthenium(III) complexes with bi-, tri- or tetradentate Schiff-base ligands [15-17]. In this continuing interest, the present report explores the coordination reaction of a series of tetradentate Schiff base ligands towards ruthenium(II) precursors. We disclose herein syntheses, structures and electrochemical properties of a series of ruthenium(III)-salipn and ruthenium(II)-salalipn complexes with tetradentate Schiff base ligands.

2. Experimental

2.1. *General considerations*

All synthetic manipulations were carried out under dry nitrogen by standard Schlenk techniques. Solvents were purified by standard procedures and distilled prior to use. Triethylamine, 1,2-diaminopropane, salicylaldehyde, 3,5-dibromosalicylaldehyde and 5-chlorosalicylaldehyde were purchased from Alfa Aesar Ltd. and used without purification. The N_2,O_2-tetradentate Schiff bases were prepared by the condensation between 1,2-diaminopropane and according

salicylaldehyde in refluxing ethanol [18]. $[Ru(PPh_3)_3Cl_2]$ [19] and $[RuHCl(CO)(PPh_3)_3]$ [20] were prepared according to the literature methods. NMR spectra were recorded on a Bruker ALX 400 Plus spectrometer operating at 400 MHz for ^1H and 162 MHz for ^{31}P. Chemical shifts (δ, ppm) were reported with reference to $SiMe_4$ (^1H) and H_3PO_4 (^{31}P). Infrared spectra were recorded on a Perkin-Elmer 16 PC FT-IR spectrophotometer with the use of pressed KBr pellets and positive FAB mass spectra were recorded on a Finnigan TSQ 7000 spectrometer. Elemental analyses were carried out using a Perkin-Elmer 2400 CHN analyzer. Cyclic voltammetry was performed with a CHI 660 electrochemical analyzer. A standard three-electrode cell was used with a glassy carbon working electrode (Φ = 3 mm), a platinum counter electrode and an Ag/AgCl reference electrode under nitrogen atmosphere at 25 °C. Formal potentials (E^o) were measured in CH_2Cl_2 solutions with 0.1 M $[^nBu_4N]PF_6$ as supporting electrolyte and reported with reference to the ferrocenium–ferrocene couple ($Cp_2Fe^{+/0}$, $E_{1/2}$ = 0.56 V). In the –1.5 to +1.5 V region, a potential scan rate of 100 mV s^{-1} was used.

2.2. *Synthesis of chloro-(N,N'-bis(salicylidene)-1,2-(1-methyl)ethane diaminato)-triphenylphosphine-ruthenium(III) dichloromethane solvate $[Ru^{III}Cl(PPh_3)(salipn)]\cdot 1.5CH_2Cl_2$ (1·1.5CH_2Cl_2)*

A mixture of H_2salipn (28.2 mg, 0.100 mmol) and $[Ru(PPh_3)_3Cl_2]$ (95.8 mg, 0.100 mmol) in THF (30 mL) was refluxed with stirring for 6 h, during which there was a color change from brown to dark green. The solvent was evaporated *in vacuo*, and the residue was washed with diethyl ether (5 mL × 2) and hexane (5 mL × 2). Recrystallization from CH_2Cl_2/hexane afforded black block crystals of **1**·1.5CH_2Cl_2 in seven days. Yield: 33.4 mg, 55.6% (based on Ru). IR (KBr disc, cm^{-1}): 1594 ($\nu_{C=N}$), 1314 (ν_{Ar-O}); MS (FAB): *m*/*z* 679 [M^+], 644 [M^+ – Cl], 417 [M^+ – PPh_3]. *Anal*. Calcd. for $C_{35}H_{31}N_2O_2PClRu\cdot 1.5(CH_2Cl_2)$ (%): C, 54.41; H, 4.26; N, 3.48. Found: C, 54.47; H, 4.23; N, 3.50.

2.3. *Synthesis of chloro-(N,N'-bis(3,5-dibromosalicylidene)-1,2-(1-methyl)ethane diaminato)-triphenylphosphine-ruthenium(III) $[Ru^{III}Cl(PPh_3)(salipn\text{-}Br_4)]$ (2)*

A mixture of H_2salipn-Br_4 (59.7 mg, 0.100 mmol) and $[Ru(PPh_3)_3Cl_2]$ (95.8 mg, 0.100 mmol) in THF (30 mL) was refluxed with stirring for 6 h, during which there was a color change from brown to dark red brown. The solvent was evaporated *in vacuo*, and the residue was washed with

diethyl ether (5 mL×2) and hexane (5 mL×2). Recrystallization from CH_2Cl_2/hexane afforded yellow crystals of **2** in five days. Yield: 51.0 mg, 55.6% (based on Ru). IR (KBr disc, cm^{-1}): 1654 ($\nu_{C=N}$), 1261 (ν_{Ar-O}); MS (FAB): *m*/*z* 991 [M^+], 956 [M^+ – Cl], 729 [M^+ – PPh_3]. *Anal*. Calcd. for $C_{35}H_{27}N_2O_2PBr_4ClRu$ (%): C, 42.39; H, 2.75; N, 2.83. Found: C, 42.43; H, 2.73; N, 2.86.

2.4. *Synthesis of carbonyl-(4-chloro-6-(((5-chloro-2-oxybenzyl)amino)isopropyl)-imino)methyl)phenolato)-triphenylphosphine-ruthenium(II) dichloromethane solvate [Ru^{II}(CO)(PPh_3)(salalipn-Cl_2)]·0.5CH_2Cl_2 (**3**·0.5CH_2Cl_2)*

To a solution of H_2salipn-Cl_2 (35.2 mg, 0.100 mmol) in EtOH (15 mL) was added $RuHCl(CO)(PPh_3)_3$ (950 mg, 0.100 mmol) in THF(15 mL), and then triethylamine (Et_3N) (10.1 mg, 0.100 mmol) was introduced. The reaction mixture was stirred for 9 h at 90 °C, during which the color of solution changed from reddish grey to bright yellow green. After removal of solvents *in vacuo*, the residue was washed with diethyl ether (5 mL×2) and hexane (5 mL×2) to give the desired product. Recrystallization from CH_2Cl_2/hexane afforded yellow crystals of **3**·0.5CH_2Cl_2 for X-ray diffraction in a week. Yield: 37.4 mg, 50.7% (based on Ru). ^{1}H NMR (400 MHz, $CDCl_3$): δ 1.23 (d, *J* = 8.0 Hz, 3H, C*H*$_3$), 2.50 (m, 1H, N*H*), 2.77-3.15 (m, 5H, 2C*H*$_2$ + C*H*), 6.60–6.63 (m, 2H, Ar), 7.06–7.12 (m, 4H, Ar), 7.38–7.43 (m, 10H, P*Ph*), 7.94-8.05 (m, 6H, *H*C=N + P*Ph*) ppm. ^{31}P NMR (162 MHz, $CDCl_3$): 29.43 ppm. IR (KBr disc, cm^{-1}): 1638 ($\nu_{C=N}$), 1945 ($\nu_{C\equiv O}$), 3280 (ν_{N-H}). MS (FAB): *m*/*z* 741 [M^+], 713 [M^+ – CO], 479 [M^+ – PPh_3]. *Anal*. Calcd. for $C_{36}H_{30}N_2O_3PCl_2Ru$·0.5($CH_2Cl_2$) (%): C, 58.30; H, 4.08; N, 3.78. Found: C, 58.34; H, 4.04; N, 3.81.

2.5. *Synthesis of carbonyl-(2,4-dibromo-6-(((3,5-dibromo-2-oxybenzyl)amino)isopropyl)-imino)methyl)phenolato)-triphenylphosphine-ruthenium(II) [Ru^{II}(CO)(PPh_3)(salalipn-Br_4)] (**4**)*

To a slurry of [$RuHCl(CO)(PPh_3)_3$] (950 mg, 0.100 mmol) in THF (15 mL) was added a solution of H_2salipn-Br_4 (59.8 mg, 0.100 mmol) and Et_3N (10.1 mg, 0.100 mmol) in EtOH (15 mL), and then the mixture was heated at 90 °C with stirring 10 h, during which there was a color change from reddish grey to bright yellow green. After removal of solvents *in vacuo*, the residue was washed with diethyl ether (5 mL×2) and hexane (5 mL×2) to give the desired product, which was

recrystallized from CH_2Cl_2/hexane. Yellow block-shaped crystals of **4** were harvested in five days. Yield: 51.2 mg, 51.8% (based on Ru). ^{1}H NMR (400 MHz, $CDCl_3$): δ 1.23 (d, *J* = 8.0 Hz, 3H, C*H*$_3$), 2.52 (br, 1H, N*H*), 2.78-3.19 (m, 5H, 2C*H*$_2$ + C*H*), 6.68 (d, *J* = 4.0 Hz, 1H, Ar), 7.16 (d, *J* = 4.0 Hz, 1H, Ar), 7.38–7.42 (m, 10H, P*Ph*), 7.69–7.78 (m, 2H, Ar), 7.96-8.05 (m, 6H, *H*C=N + P*Ph*) ppm. ^{31}P NMR (162 MHz, $CDCl_3$): 31.15 ppm. IR (KBr disc, cm^{-1}): 1640 ($\nu_{C=N}$), 1947 ($\nu_{C\equiv O}$), 3287 (ν_{N-H}). MS (FAB): *m*/*z* 986 [M^+], 958 [M^+ – CO], 724 [M^+ – PPh_3]. *Anal*. Calcd. for $C_{36}H_{29}N_2O_3PBr_4Ru$ (%): C, 43.82; H, 2.84; N, 3.78. Found: C, 43.86; H, 2.82; N, 3.82.

2.6. *X-ray crystallography*

A summary of crystallographic data and experimental details for **1**·1.5CH_2Cl_2, **2**, **3**·0.5CH_2Cl_2 and **4** are summarized in table 1 and their selected bond lengths and angles are collected in table 2 for comparison. Intensity data were collected on a Bruker SMART APEX 2000 CCD diffractometer using graphite-monochromated Mo-Kα radiation (λ = 0.71073 Å) at 296(2) K. The collected frames were processed with SAINT [21]. The data was corrected for absorption using SADABS [22]. Structures were solved by the direct methods and refined by full-matrix least-squares on F^2 using the SHELXTL software package [23, 24]. All non-hydrogen atoms were refined anisotropically. The positions of all hydrogens were generated geometrically (C_{sp3}–H = 0.96 and C_{sp2}–H = 0.93 Å) and included in the structure factor calculations with assigned isotropic thermal parameters, but were not refined.

3. Results and discussion

As shown in scheme 1, treatment of $[RuCl_2(PPh_3)_3]$ with equal equiv. tetradentate Schiff base H_2Salen or H_2Salen-Br_4 in the presence of triethylamine in THF afforded the expected ruthenium(III) complexes $[Ru^{III}Cl(PPh_3)$(salipn)] (**1**) and $[Ru^{III}Cl(PPh_3)$(salipn-Br_4)] (**2**), respectively. Two triphenylphosphine and one chlorido ligand in the starting ruthenium(II) complex $[RuCl_2(PPh_3)_3]$ were replaced by the salipn-type ligand in the present reaction system, thus, the tetradentate dianionic O_2,N_2-ligands bind the ruthenium center facially. Oxidation of ruthenium(II) to ruthenium(III) by air took place during formation of **1** and **2**, similar to that in preparation of the related complexes $[RuCl(PPh_3)$(salen)], $[RuCl(PPh_3)$(salphen)], $[RuCl(PPh_3)$(salcyn)], *et al*. by reaction of $[RuCl_2(PPh_3)_3]$ and respective tetradentate Schiff

bases [6-9, 16, 25]. Interactions of [RuHCl(CO)(PPh_3)$_3$] with one equivalent of H_2salipn-Cl_2 or H_2salipn-Br_4 in the presence of triethylamine led to isolation of [Ru^{II}(CO)(PPh_3)(salalipn-Cl_2)] (**3**) and [Ru^{II}(CO)(PPh_3)(salalipn-Br_4)] (**4**), respectively, in moderate yields. One of the imine bonds was nucleophilically attacked by hydride to result in the formation of a mixed imine-amine ligand salalipn (see chart 1) in complexes **3** and **4**, which is similar to that in our previous report involved in reaction of [RuHCl(CO)(PPh_3)$_3$] and *N*,*N'*-disalicylidene-1,2-phenylenediamine [25]. It has been noted that this *in situ* ligand reduction was also observed between reactions of [M(CO)$_2$(PPh_3)$_2Cl_2$] (M = Ru, Os) and a carbohydrate derived salen ligand, and the authors stated that PPh_3 may act as a reducing agent [26].

IR spectra of Schiff base ligands in **1**-**4** showed strong bands in the region of 1599–1654 cm^{-1} which are characteristic of the CH=N group absorptions. The weak bands at around 3280 cm^{-1} in the IR spectra of **3** and **4** may be tentatively assigned to the ν(N–H) absorption. The C≡O stretching vibration modes were found at *ca.* 1945 cm^{-1} in the IR spectra of ruthenium(II) carbonyl complexes **3** and **4**, similar to those in related ruthenium(II) carbonyl triphenylphosphine complexes [27]. Complexes **1** and **2** had no NMR signals, indicating they are paramagnetic species and the oxidation state of the ruthenium center is +3. In the ^{1}H NMR spectra of unsymmetrical free ligands H_2salipn-Cl_2 and H_2salipn-Br_4, there were two aldimine (–C*H*=N–) proton resonances at around 8.20 ppm as two singlets. The methyl protons exhibited as a doublet at about 1.42 ppm with J = 8.0 Hz. The phenolic protons appear at 13.15 ppm for H_2salipn-Cl_2 and 14.20 ppm for H_2salipn-Br_4, which could not be observed in the ^{1}H NMR spectra of **3** and **4**. Some new signals appeared in the region at about 2.50 ppm that correspond to amine N*H* protons. This suggests that one of the imine groups in ligands is hydrogenated during the complex formation [28]. Moreover, the ^{31}P{^{1}H} NMR spectra of **3** and **4** exhibit a singlet at δ29.43 and 31.15 ppm, respectively, which are comparable to that in the starting material [RuHCl(CO)(PPh_3)$_3$] (39.06, 29.11 ppm). The positive ion FAB mass spectra of **1**-**4** display the expected peaks corresponding to the molecular ions {[M^+], [M^+ – Cl], [M^+ – CO] and [M^+ – PPh_3] with the characteristic isotopic distribution patterns.

The structures of **1**·1.5CH_2Cl_2, **2**, **3**·0.5CH_2Cl_2 and **4** have been established by X-ray crystallography. The perspective views of the molecular structures of **1**-**4** are shown in figures 1-4, respectively, with atom numbering schemes. According to the X-ray structures the salipn

ligand in **1**·1.5CH_2Cl_2 and salipn-Br_4 ligand in **2** coordinate to ruthenium atoms in a tetradentate mode. The two phenolic oxygen atoms and the two imine nitrogen atoms of the Schiff-base constitute the basal plane in **1**·1.5CH_2Cl_2 and **2**, while the chlorine and phosphine atoms occupy the axial positions. The Cl–Ru–P bond angles are 176.89(4)° in **1**·1.5CH_2Cl_2 and 176.45(14)° in **2**, which are comparable to those in related ruthenium-N_2,O_2 complexes [$Ru^{III}Cl(PPh_3)$(salphen)] (175.08(2)°) [25], [$Ru^{III}Cl(PPh_3)$(salcyn)] (173.7(3)°) [6] and similar to that in the previously reported complex [$Ru^{III}Cl(PPh_3)$(salipn)]·2CH_2Cl_2 (176.06(7)°) [16]. In ruthenium(II) carbonyl complexes **3**·0.5CH_2Cl_2 and **4**, the two phenolic oxygen atoms, one imine nitrogen atom and one amine nitrogen atom of salalipn-Cl_2 ligand in **3**·0.5CH_2Cl_2 and salalipn-Br_4 ligand in **4** also bind ruthenium centers in a tetradentate manner. However, the four atoms of salalipn-type ligands are not in the equatorial plane; instead it is coordinated in a *cis*-β fashion (chart 1) with one of the π-donating phenolato groups coordinated *trans* to the π-accepting carbonyl and the other *trans* to the σ-donating amine. As a result, the σ-donating phosphine is coordinated *trans* to the imine. The corresponding P–Ru–N bond angles are 179.57(8)° in **3**·0.5CH_2Cl_2 and 178.50(16)° in **4**. It has been noted that the carbohydrate derived Ru/Os-Salalen complexes [26] and the ruthenium complex [Ru(salbinapht)(CO)(P*i*-Pr_3)] {salbinapht = 2-[({2'-[(2-hydroxy-benzyl)-amino]-[1,1'-bi-naphthalen]-2-yl}imino)-methyl]phenolato} [28], the phosphine atom and the amine nitrogen atom are *trans* to each other. The C(8)–N(1) bond lengths are 1.488(4) and 1.496(7) Å in **3** and **4**, respectively, suggesting their C–N single bond character; while the C(12)–N(2) bond lengths are 1.283(4) Å in **3** and 1.266(7) Å in **4**, indicating their original C=N bond property. Two Ru–N bonds have almost similar bond lengths in **1**·1.5CH_2Cl_2 (1.983(3) and 2.008(3) Å) and **2** (1.965(6) and 1.981(6) Å), which are a little shorter than those in Ru-salalipn complexes **3**·0.5CH_2Cl_2 (2.125(3) and 2.054(3) Å) and **4** (2.145(4) and 2.062(5) Å). The Ru–P of 2.259(2) Å and Ru–Cl of 2.196(4) Å in **2** are shorter than those in **1**·1.5CH_2Cl_2 (2.3547(13), 2.4587(13) Å) possibly due to the Br_4 substitute effect on the salalipn ligands. The Ru–P bond lengths are 2.3592(9) Å and 2.3697(7) Å in **3**·0.5CH_2Cl_2 and **4**, respectively, comparable to that in the related ruthenium carbonyl triphenylphosphine complex [Ru^{II}(CO)(PPh_3)(salalphen)] (2.345 Å) [25].

Cyclic voltammograms for **1**-**4** scanning from −1.50 to +1.50 V are shown in figure 5. Table 3 summarizes the electrochemical data of the ruthenium(III)-salipn and ruthenium(II)-

salalipn complexes. The ruthenium(III) complexes **1** and **2** show one quasi-reversible reductive couple at about –0.80 V and one oxidative couple at around 0.67 V, which are comparable to the related ruthenium(III) complex [RuCl(PPh_3)(salen)] (–0.22 V, 0.95 V) [9]. The ruthenium(II) complexes **3** and **4** have similar quasi-reversible Ru^{II}/Ru^{III} couples (–0.74 V) compared to those of **1** and **2** (–0.80 V). Complexes **3** and **4** exhibit one weak oxidation couple at about 1.00 V, which is a little higher than those for **1** and **2** (0.67 V), an indication of the carbonyl stability of the ruthenium(II) complexes.

In summary, a series of ruthenium(II)/(III) complexes with unsymmetrical tetradentate Schiff base ligands were synthesized by reactions of ruthenium(II) starting materials [$RuCl_2(PPh_3)_3$]/[$RuHCl(CO)(PPh_3)_3$] and the corresponding free Schiff bases in the presence of organic base. Though these salipn ligands have been employed in many transition metal complexes, such as iron, manganese and vanadium [29-31], they have not yet been used to coordinate to ruthenium metal. The isolation of ruthenium complexes **1**-**4** enriched the exploration of such ligands. Formation of **1** and **2** involved in the oxidation of ruthenium(II) to ruthenium(III) by air [6]. *In situ* ligand reduction was observed in the syntheses of **3** and **4**; this imine amine transformation was also reported in other ruthenium-salen complexes [25, 26]. It is interesting to note that the mixed imine-amine ligands salalipn-Br_4 and salalipn-Cl_2 in according complexes **3** and **4** coordinated to ruthenium atoms in a *cis*-β fashion (chart 1), which resulted in the carbonyl and the phosphine *cis* to each other with the bond angles of C–Ru–P being about 87.6°.

Supplementary material

Crystallographic data for [$Ru^{III}Cl(PPh_3)$(salipn)]·1.5CH_2Cl_2 (**1**·1.5CH_2Cl_2), [$Ru^{III}Cl(PPh_3)$(salipn-Br_4)] (**2**), [$Ru^{II}(CO)(PPh_3)$(salalipn-Cl_2)]·0.5CH_2Cl_2 (**3**·0.5CH_2Cl_2) and [$Ru^{II}(CO)(PPh_3)$(salalipn-Br_4)] (**4**) have been deposited with the Cambridge Crystallographic Data Centre as supplementary publication nos. CCDC 1865332, 1865333, 1865334 and 1865335, respectively. Copies of the data can be obtained free of charge on application to CCDC, 12 Union Road, Cambridge CB2 1EZ, UK [Fax: (+44)1233-336-033; E-mail: deposit@ccdc.cam.ac.uk].

Acknowledgements

This project was supported by the Natural Science Foundation of China (21372007).

References

[1] X. Liu, C. Manzur, N. Novoa, S. Celedon, D. Carrillo, J.R. Hamon. *Coord. Chem. Rev.*, **357**, 144 (2018).

[2] W. Al Zoubi, Y.G. Ko. *J. Organomet. Chem.*, **822**, 173 (2016).

[3] P. Das, W. Linert. *Coord. Chem. Rev.*, **311**, 1 (2016).

[4] G.-Y. Li, J. Zhang, P.W.H. Chan, Z.-J. Xu, N. Zhu, C.M. Che. *Organometallics*, **25**, 1676 (2006).

[5] R. Prabhakaran, R. Huang, K. Natarajan. *Inorg. Chim. Acta*, **359**, 3359 (2006).

[6] K. Nakajima, Y. Ando, H. Mano, M. Kojima. *Inorg. Chim. Acta*, **274**, 184 (1998).

[7] W.-H. Leung, C.M. Che. *Inorg. Chem.*, **28**, 4619 (1989).

[8] F. Pointillart, K. Bernot, L. Sorace, R. Sessoli, D. Gatteschi. *Dalton Trans.*, 2689 (2007).

[9] F. Pointillart, Y. L. Gal, S. Golhen, O. Cador, L. Ouahab. *Inorg. Chem.*, **47**, 9730 (2008).

[10] H. Fujita, T. Uchida, R. Irie, T. Katsuki. *Chem. Lett.*, **36**, 1092 (2007).

[11] D.A. Atwood, J.A. Jegier, N.F. Lindholm, K.J. Martin, D. Rutherford. *J. Coord. Chem.*, **38**, 305 (1996).

[12] T. Storr, P. Verma, Y. Shimazaki, E.C. Wasinger, T.D.P. Stack. *Chem. Eur. J.*, **16**, 8980 (2010).

[13] J.E. Ziegler, G. Du, P.E. Fanwick, M.M. Abu-Omar. *Inorg. Chem.*, **48**, 11290 (2009).

[14] S.R. Lane, N. Sisay, B. Carney, S. Dannoon, S. Williams, H.P. Engelbrecht, C.L. Barnes, S.S. Jurisson. *Dalton Trans.*, **40**, 269 (2011).

[15] C.-J. Wang, W.-F. Xu, B.-H. Tong, A.-Q. Jia, Q.-F. Zhang. *J. Coord. Chem.*, **70**, 1617 (2017).

[16] L.H. Tang, F. Wu, H. Lin, A.-Q. Jia, Q.-F. Zhang. *Inorg. Chim. Acta*, **477**, 212 (2018).

[17] F. Wu, C.-J. Wang, H. Lin, A.-Q. Jia, Q.-F. Zhang. *J. Coord. Chem.*, **71**, 219 (2018).

[18] X.-F. Yin, H. Lin, A.-Q. Jia, Q. Chen, Q.-F. Zhang. *J. Coord. Chem.*, **66**, 3229 (2013).

[19] T.A. Stephenson, G. Wilkinson. *J. Inorg. Nucl. Chem.*, **28**, 945 (1966).

[20] U. Koelle, J. Kossakowski. *Inorg. Synth.*, **29**, 225 (1992).

[21] *SMART and SAINT+ for Windows NT Version 6.02a*. Bruker Analytical X-ray Instruments Inc., Madison, Wisconsin, USA (1998).

[22] G.M. Sheldrick, *SADABS*, University of Göttingen, Germany (1996).

[23] G.M. Sheldrick. *Acta Crystallogr., Sect. A*, **64**, 112 (2008).

[24] G.M. Sheldrick. *Acta Crystallogr., Sect. C*, **71**, 3 (2015).

[25] Y. Li, Q. Ma, H.-T. Shi, Q. Chen, Q.-F. Zhang. *Z. Naturforsch., B*, **66**, 324 (2011).

[26] S. Mandal, S. Mandal, D.K. Seth, B. Mukhopadhyay, P. Gupta. *Inorg. Chim. Acta*, **398**, 83 (2013).

[27] A. Sharmin, R.C. Darlington, K.I. Hardcastle, M. Ravera, E. Rosenberg, J.B. Alexander Ross. *J. Organomet. Chem.*, **694**, 988 (2009).

[28] F.F. van de Watering, M. Lutz, W.I. Dzik, B. de Bruin, J.N.H. Reek. *ChemCatChem*, **8**, 2752 (2016).

[29] P.B. Chatterjee, D. Mandal, A. Audhya, K.-Y. Choi, A. Endo, M. Chaudhury. *Inorg. Chem.*, **47**, 3709 (2008).

[30] J. Adhikary, A. Datta, S. Dasgupta, A. Chakraborty, M.I. Menéndez, T. Chattopadhyay. *RSC Adv.*, **5**, 92634 (2015).

[31] E. Gungor, Y. Yahsi, H. Kara, A. Caneschi. *CrystEngComm*, **17**, 3082 (2015).

Graphical abstract

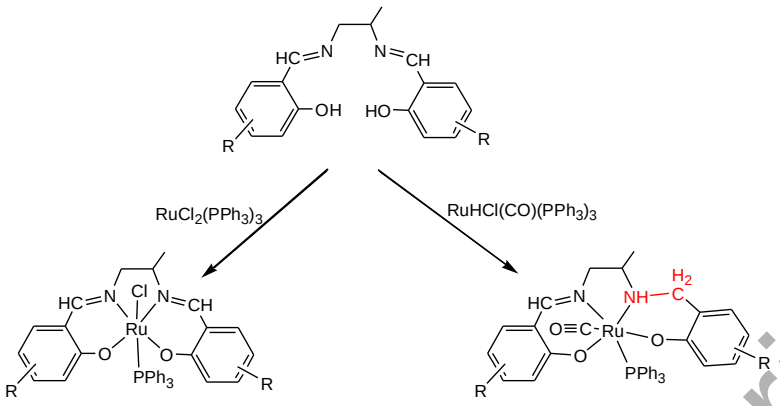

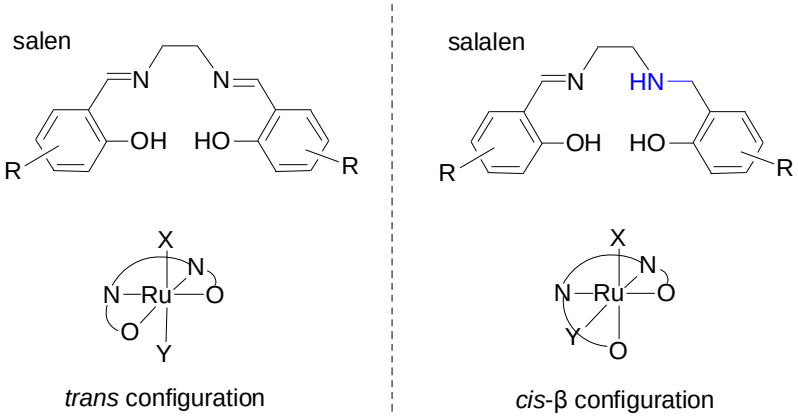

Chart 1. Structures of salen and salalen ligands and their derivatives.

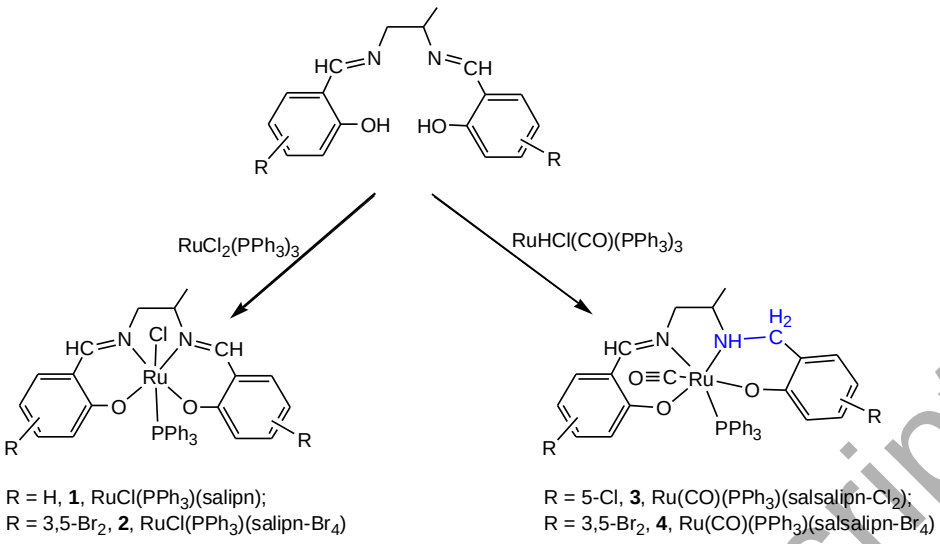

R = H, **1**, $RuCl(PPh_3)$(salipn);
R = 3,5-Br_2, **2**, $RuCl(PPh_3)$(salipn-Br_4)

R = 5-Cl, **3**, $Ru(CO)(PPh_3)$(salsalipn-Cl_2);
R = 3,5-Br_2, **4**, $Ru(CO)(PPh_3)$(salsalipn-Br_4)

Scheme 1. Syntheses of **1**-**4**.

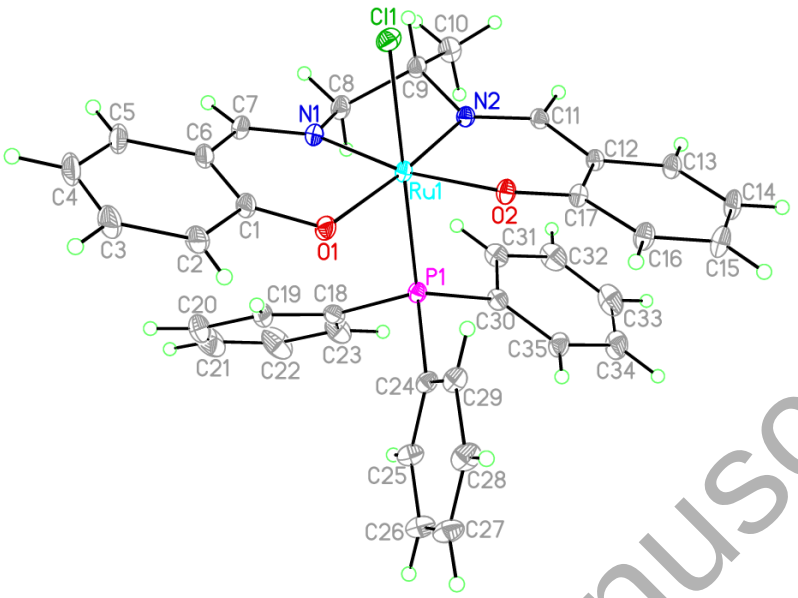

Figure 1. ORTEP diagram of [RuCl(PPh_3)(salipn)] (**1**) showing the atom labeling scheme and 40% thermal ellipsoids. Hydrogens and solvents are omitted for clarity.

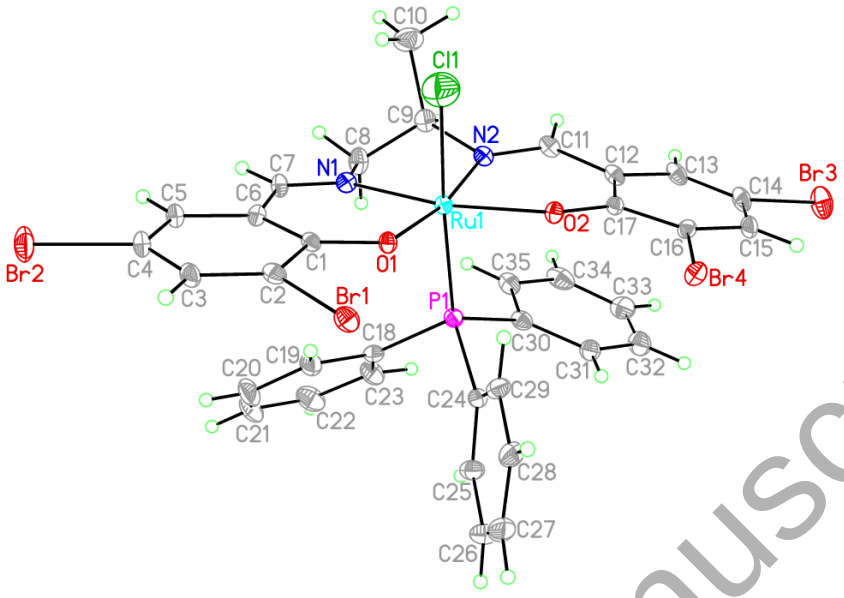

Figure 2. ORTEP diagram of [RuCl(PPh_3)(salipn-Br_4)] (**2**) showing the atom labeling scheme and 40% thermal ellipsoids. Hydrogens are omitted for clarity.

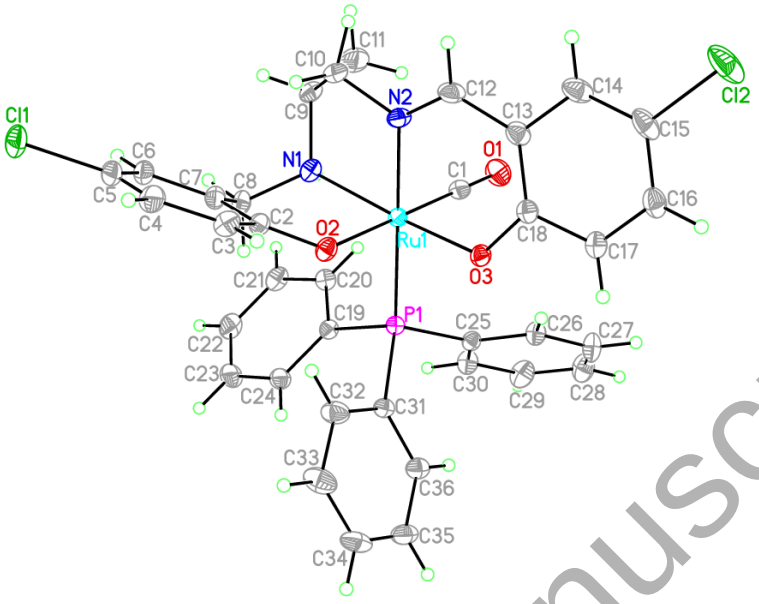

Figure 3. ORTEP diagram of [Ru(CO)(PPh_3)(salalipn-Cl_2)] (**3**) showing the atom labeling scheme and 40% thermal ellipsoids. Hydrogens and the solvent are omitted for clarity.

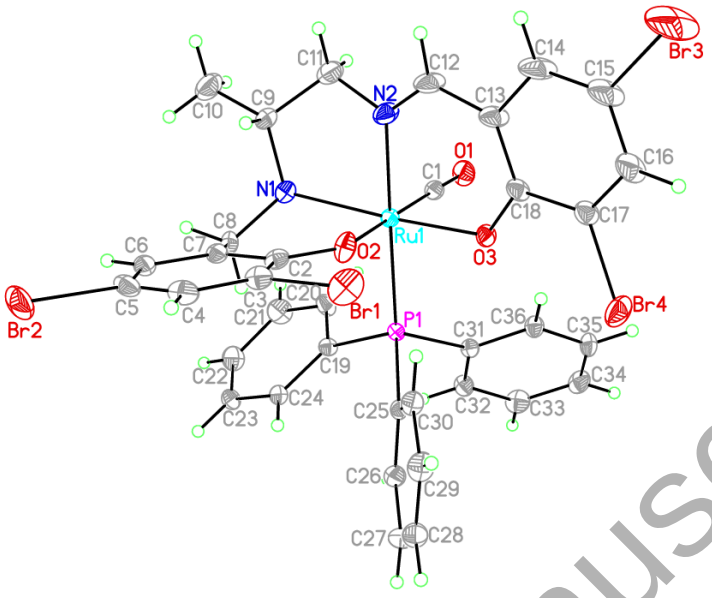

Figure 4. ORTEP diagram of [Ru(CO)(PPh_3)(salalipn-Br_4)] (**4**) showing the atom labeling scheme and 40% thermal ellipsoids. Hydrogens are omitted for clarity.

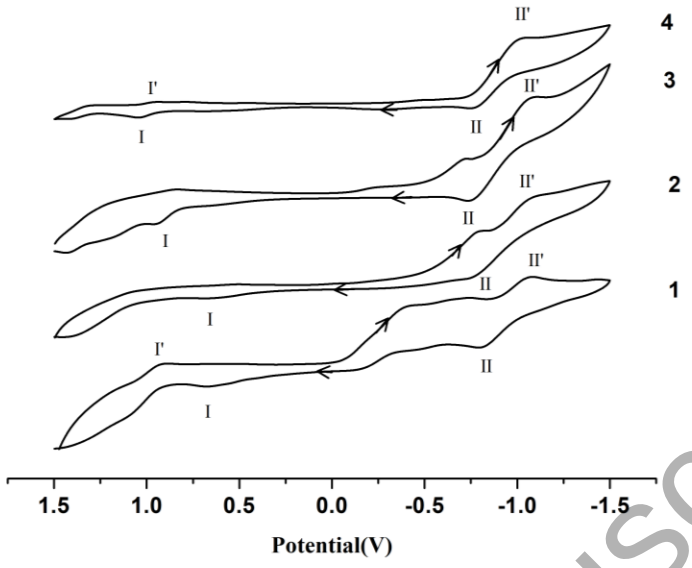

Figure 5. Cyclic voltammogram of **1**-**4** (0.001 M) in CH_2Cl_2 at 25 °C at 100 mV s^{-1} scan rate with 0.1 M [$^{n}Bu_4N$]PF_6 as supporting electrolyte.

Table 1. Crystallographic data and experimental details for $[Ru^{III}Cl(PPh_3)(salipn)]\cdot 1.5CH_2Cl_2$ (**1**·$1.5CH_2Cl_2$), $[Ru^{III}Cl(PPh_3)(salipn\text{-}Br_4)]$ (**2**), $[Ru^{II}(CO)(PPh_3)(salalipn\text{-}Cl_2)]\cdot 0.5CH_2Cl_2$ (**3**·$0.5CH_2Cl_2$) and $[Ru^{II}(CO)(PPh_3)(salalipn\text{-}Br_4)]$ (**4**).

Complex	**1**·$1.5CH_2Cl_2$	**2**	**3**·$0.5CH_2Cl_2$	**4**
Empirical formula	$C_{36.5}H_{34}N_2O_2PCl_4Ru$	$C_{35}H_{27}N_2O_2PBr_4ClRu$	$C_{36.5}H_{32}N_2O_3PCl_3Ru$	$C_{36}H_{29}N_2O_3PBr_4Ru$
Formula weight	806.49	994.72	785.03	989.29
Crystal system	Monoclinic	Monoclinic	Monoclinic	Triclinic
a (Å)	12.896(5)	13.9571(11)	9.138(2)	12.8542(10)
b (Å)	13.995(6)	17.5871(15)	30.118(8)	13.3858(11)
c (Å)	21.578(9)	14.9296(12)	13.368(3)	13.6434(11)
α (°)				100.5026(10)
β (°)	98.685(6)	109.0377(11)	100.387(3)	114.6044(9)
γ (°)				112.1851(10)
V (Å^3)	3850(3)	3464.2(5)	3618.7(16)	1808.6(3)
Space group	$P2_1/n$	$P2_1/n$	$P2_1/c$	$P\bar{1}$
Z	4	4	4	2
D_{calc} (g cm^{-3})	1.392	1.907	1.441	1.817
Temperature (K)	296(2)	296(2)	296(2)	296(2)
F(000)	1640	1932	1596	964
μ(Mo-Kα) (mm^{-1})	0.759	5.225	0.736	4.934
Total reflns.	23494	21849	15123	11570
Independent reflns.	8749	7957	8274	8038
Parameters	434	416	438	429
R_{int}	0.0294	0.0673	0.0391	0.0182
$R1$[a], $wR2$[b] ($I > 2\sigma(I)$)	0.0537, 0.1488	0.0587, 0.1318	0.0428, 0.1056	0.0506, 0.1166
$R1$, $wR2$ (all data)	0.0775, 0.1698	0.1388, 0.1649	0.0650, 0.1183	0.0762, 0.1292
GoF[c]	1.044	0.968	1.033	1.045

[a] $R1 = \Sigma\,||F_o| - |F_c||\,/\,\Sigma|F_o|$. [b] $wR2 = [\Sigma w(|F_o^2| - |F_c^2|)^2/\Sigma w|F_o^2|^2]^{1/2}$. [c] $\mathrm{GoF} = [\Sigma w(|F_o| - |F_c|)^2/(N_{obs} - N_{param})]^{1/2}$.

Table 2. Selected bond lengths (Å) and angles (°) for **1**·1.5CH_2Cl_2, **2**, **3**·0.5CH_2Cl_2 and **4**.

Complex	Ru–N	Ru–O	Ru–P	Ru–Cl/C	N–Ru–O	N–Ru–N	O–Ru–O	N–Ru–P	O–Ru–P
1	1.983(3) 2.008(3)	2.008(3) 2.016(3)	2.3547(13)	2.4587(13)	170.63(13) 91.23(11) 90.67(13) 173.70(12)	83.05(13)	95.07(11)	96.04(11) 92.39(10)	87.72(9) 91.59(9)
2	1.965(6) 1.981(6)	2.102(4) 2.106(5)	2.259(2)	2.196(4)	169.8(2) 90.5(2) 90.6(2) 171.6(2)	84.9(3)	92.82(17)	93.37(18) 95.23(17)	96.15(13) 92.09(14)
3	2.125(3) 2.054(3)	2.071(2) 2.105(2)	2.3592(9)	1.812(3)	169.35(10) 90.98(10) 84.83(9) 87.73(10)	80.50(11)	85.14(8)	179.57(8) 99.12(9)	89.38(6) 94.95(6)
4	2.145(4) 2.062(5)	2.058(4) 2.060(3)	2.3697(12)	1.823(6)	165.88(16) 85.42(16) 91.05(16) 85.9(2)	80.46(18)	82.71(14)	178.50(16) 99.79(12)	95.61(12) 88.98(10)

Table 3. Electrochemical data for ruthenium-salipn/salalipn complexes.

Complex	E^{o},[a] V *vs.* Ag/AgCl	
	I	II
[$Ru^{III}Cl(PPh_3)$(**s**alipn)]	0.67	–0.79
[$Ru^{III}Cl(PPh_3)$(**s**alipn-Br_4)]	0.67[b]	–0.80
[$Ru^{II}(CO)(PPh_3)$(**s**alalipn-Cl_2)]	0.96[b]	–0.74
[$Ru^{II}(CO)(PPh_3)$(**s**alalipn-Br_4)]	1.05	–0.74

[a] Glassy carbon working electrode, platinum counter electrode, Ag/AgCl reference electrode, 0.1 M [$^{n}Bu_4N$]PF_6 in CH_2C1_2 as supporting electrode. Ferrocene was added as internal standard. [b] Irreversible.